Localization and Classification of Cell Nuclei in Post-Neoadjuvant Breast Cancer Surgical Specimen Using Fully Convolutional Networks

Rene Bidart[1], Mehrdad J. Gangeh[2], Mohammad Peikari[2], Sherine Salama[3], Sharon Nofech-Mozes[3], Anne L. Martel[2, 4], Ali Ghodsi[1]

[1] Department of Statistics and Actuarial Science, University of Waterloo, Waterloo, ON, Canada

[2] Departments of Medical Biophysics, University of Toronto, Toronto, ON, Canada

[3] Laboratory of Medicine and Pathobiology, University of Toronto, ON, Canada

[4] Department of Physical Sciences, Sunnybrook Research Institute, Toronto, ON, Canada

ABSTRACT

Neoadjuvant therapy (NAT) is an option for locally advanced breast cancer patients to downsize tumour allowing for less extensive surgical operation, better cosmetic outcomes, and lesser post-operative complications. The quality of NAT is assessed by pathologists after examining the tissue sections to reveal the efficacy of treatment, and also associate the outcome with the patient's prognosis. There are many factors involved with assessing the best treatment efficacy, including the amount of residual cancer within tumour bed. Currently, the process of assessing residual tumour burden is qualitative, which may be time-consuming and impaired by inter-observer variability. In this study, an automated method was developed to localize, and subsequently classify nuclei figures into three categories of lymphocyte (L), benign epithelial (BE), and malignant epithelial (ME) figures from post-NAT tissue slides of breast cancer. A fully convolutional network (FCN) was developed to perform both tasks in an efficient way. In order to find the cell nuclei in image patches (localization), the FCN was applied over the entire patch, generating four heatmaps corresponding to the probability of a pixel being the centre of an L, BE, ME, or non-cell nuclei. Non-maximum suppression algorithm was subsequently applied to the generated heatmaps to estimate the nuclei locations. Finally, the highest probability corresponding to each predicted cell nucleus in the heatmaps was used for the classification of the nucleus to one of the three classes (L, BE, or ME). The final classification accuracy on detected nuclei was 94.6%, surpassing previous machine learning methods based on handcrafted features on this dataset.

Keywords: Fully convolutional networks, pathology, localization, cell nuclei classification, heatmaps, non-maximum suppression, breast cancer

INTRODUCTION

Neoadjuvant therapy (NAT) is a treatment of choice for selected high-risk and/or locally advanced breast cancer (LABC) patients[1]. The goal of NAT is to downsize the tumour, allowing for less extensive surgical operation resulting in better cosmetic outcomes and reduced post-operative complications. Also, after NAT, the efficacy of the therapy can be assessed *in vivo* with the aim of associating the treatment response to the new therapeutic agents in drug trials and modifying the treatment for patients who show little to no response to the conventional therapies.

It is desirable to achieve pathologic complete response (pCR) after the course of NAT which indicates the absence of residual cancer in the breast tissue and associated axillary lymph nodes. A pCR is associated with better patient prognosis[2]. Currently, residual tumour burden assessment is done manually by pathologists on hematoxylin and eosin (H&E) stained tissue sections through a qualitative and time-consuming process. Although there are different scoring factors reported for assessing tumour response to NAT, the cellularity fraction of cancer within tumour bed provides a better prognostic indicator of the efficacy of the treatment compared to other factors[3].

The objective of this paper was to present an automated method based on a fully convolutional network (FCN)[4] to locate and distinguish cancer nuclei from other nuclei figures within the tissue micro-environment. Major nuclei figures within tissue microenvironment are stromal, lymphocytic (L), benign epithelial (BE), and malignant epithelial (ME) nuclei. Stromal nuclei are usually thinly elongated figures that could be identified by their much longer major axis. Therefore, the focus of this study was to distinguish ME figures from BE and L figures.

METHODS

Patient data

The dataset was obtained from H&E stained whole slide images (WSIs) of breast tissue samples from 46 patients post-neoadjuvant treatment, and was prepared and scanned at Sunnybrook Health Sciences Centre. There were 92 WSIs in the dataset that were scanned at 20× magnification (0.5 μm/pixel). Nuclei figures from three categories of L, BE, and ME were marked by an expert pathologist by clicking on the centroid of the individual nuclei within n = 148 rectangular regions of arbitrary size drawn by the pathologist. Selected regions were chosen in such a way that contained a mixture of nuclei categories. More than 27000 nuclei (m_1 = 3034 lymphocyte, m_2 = 9964 benign epithelial, and m_3 = 14314 malignant epithelial figures) were marked by the pathologist from all rectangular regions and used to assess the performance of the automated method presented in this paper.

Outline of the methodology

The pipeline for the proposed scheme was consisting of three main steps, including: 1) training an FCN to recognize three classes of cell nuclei including BE, ME, and L nuclei, as well as no cell; 2) localization of cell nuclei by applying the trained FCN in previous step to generate four heatmaps of the probability of each nuclei class, including no nuclei class, followed by a non-maximum suppression algorithm to estimate nuclei locations ; and 3) classification of the cell nuclei at predicted cell nuclei locations.

Training an FCN model to recognize cell nuclei subtypes

In order to perform cell nuclei localization, a network needed to be trained first to recognize different cell classes in addition to no-cell class. To this end, a training dataset was created consisting of tiles that each included nuclei of one class, or no nucleus (see Fig. 1 for examples of tiles on four classes). The tiles were created by taking a box of fixed size around each nucleus, centred at the pathologist's annotations. Since there could be more than one nucleus in each tile, the FCN was trained based on the nucleus at the centre of a tile. Tiles of non-cell tissues were created by randomly selecting points that were at least 5 μm (10 pixels) from any other cell. Including no-cell class (tiles) in the training set would enable the trained FCN to perform localization as well.

Cell nuclei localization

The trained FCN in previous step was applied to the input images to generate the probability of a nucleus being centred at that location, in addition to the class probabilities of that nucleus. By applying the trained FCN across an entire image, four heatmaps were generated for each image corresponding to each of the cell probabilities, including the probability of no cell. An example for the heatmaps generated for an image is shown in Fig. 2. By looking at $1 - p(\text{no cell}^*)$, the probability of there being a cell in any location could be explicitly obtained. This produced heatmaps that indicated the probability of a given pixel being the center of a nucleus. In order to convert the four heatmaps generated in the previous step into a set of cell nuclei locations, a non-maximum suppression algorithm was employed. This relied on the fact that the points on the cell probability heatmaps corresponding to the highest probability were most likely to be the centre of the cells. In this procedure, the pixels with the highest cell probability were iteratively found, and then all points within a radius r of these pixels were set to 0.

* This was the main reason that the non-cell data was added as a class for the training the FCN.

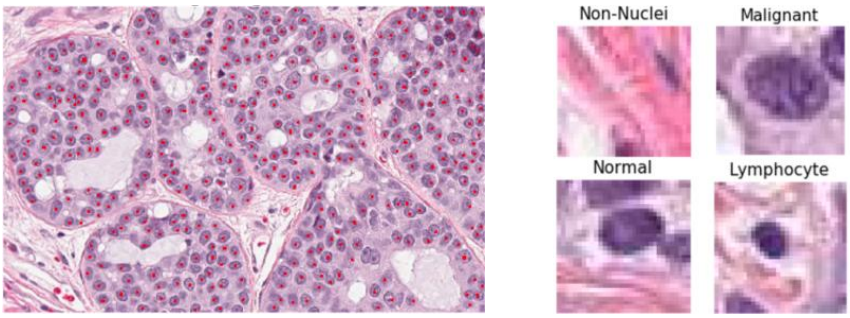

(a) (b)

Fig. 1- (a) Subsection of H&E stained slide, taken at 20× magnification, showing the malignant nuclei labeled in red (b) examples of extracted nuclei (tiles) from the image patch. Each tile is 32×32 pixels (16 μm×16 μm).

Classification of cell nuclei at predicted locations

After estimation of cell nuclei locations in previous step, the class labels (L, BE, or ME) for the predicted locations was assigned based on the corresponding highest probability from the heatmaps for those points.

Remarks on the implementations

The data was divided to three sets: 60% for training, 15% for validation (tuning the hyper-parameters and model selection), and 25% for testing the network. The implementation of the network was accomplished using the TensorFlow library[5]. A fully convolutional network with two inception modules[6] was used. That is, for the final layer, instead of fully connected layers, a convolutional kernel that spanned the full width of the feature map was employed with no zero padding. The output from the network consisted of four convolutional feature maps, corresponding to the class probabilities. The main reason for using a fully convolutional network was to enable varying sized inputs, resulting in faster predictions at test time. When the network was tested on a larger image than what was used during training, it would output multiple probabilities corresponding to the spatial locations of the image. Other design criteria included the augmentation of the data for training the network, the size of input tiles for training and testing, normalization of the inputs, regularization of the network using dropout, the number of layers for the convolutional network, and the size of radius *r* in the non-maximum suppression algorithm, which were all selected by tuning the network on a validation set. The test set remained unseen during these hyper-parameter tuning and model selection.

RESULTS

Fig. 2 depicts the heatmaps generated for a sample input image to the network. Table 1 presents the classification accuracy, sensitivity, and specificity achieved by the proposed method on the test set. The results were compared with a machine learning method based on handcrafted features. The rival method consisted of segmentation of nuclei figures using decorrelation stretching technique[7], feature extraction based on extracted textural, morphological, and spatial features to describe the nuclei figures properties, and a support vector machine (SVM) with radial basis function (RBF) kernel as the classifier. The rival method was labeled as SVM in Table 1. As can be observed from these results, the proposed method based on a fully convolutional network boosted the performance on the classification of the cell nuclei at predicted locations compared to the handcrafted features.

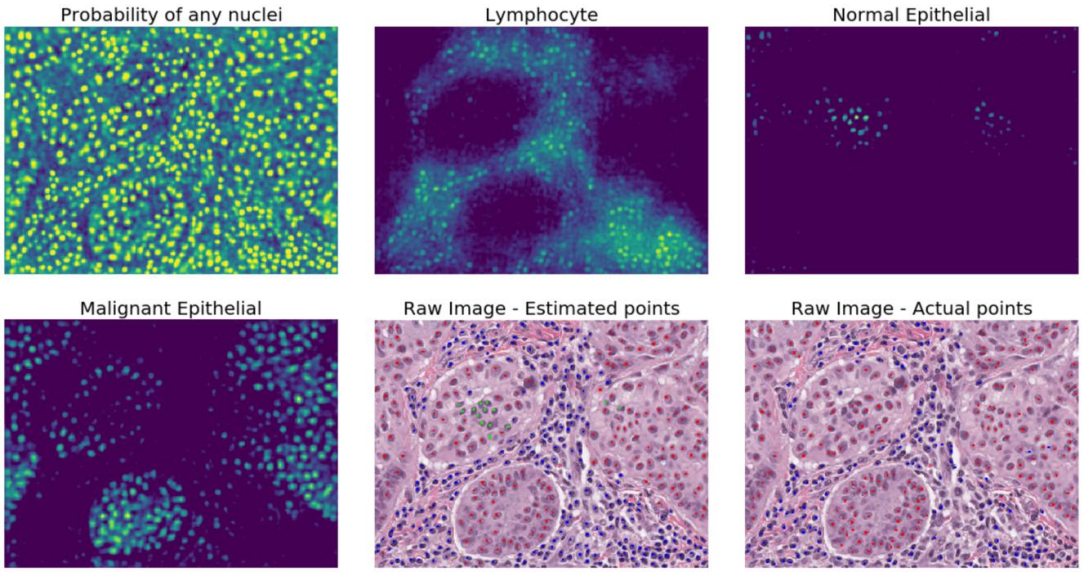

Figure 2- Representative heatmaps produced by the network for a typical input image, and the predictions on the raw image. L, BE, and ME nuclei are shown as blue, green and red dots, respectively (the images should be digitally enlarged for the best view).

Table 1-The performance of the proposed network in comparison with handcrafted features on the test set

Class	Accuracy (%)		Sensitivity (%)		Specificity (%)	
	FCN	SVM	FCN	SVM	FCN	SVM
L	99	92	93	80	100	94
BE	95	75	99	50	94	92
ME	95	77	93	91	99	63

Abbreviations: L: Lymphocyte
BE: Benign Epithelial
ME: Malignant Epithelial
FCN: Fully Connected Network (proposed approach)
SVM: The rival method based on handcrafted features and SVM classifier

CONCLUSIONS

A fully convolutional network equipped with inception modules was designed to localize and classify cell nuclei in post-neoadjuvant therapy tissue slides of breast cancer. The proposed network accurately localized the cell nuclei using a pre-trained network, and based on the generation of heatmaps of probability of each nuclei class followed by a non-maximum suppression algorithm. The predicted cell nuclei locations were subsequently classified as lymphocyte, benign epithelial or malignant epithelial with high accuracy, sensitivity, and specificity. The results validated the viability of the proposed approach in this application for the first time, particularly in comparison with handcrafted features.

REFERENCES

[1] Faneyte, I.F., Schrama, J.G., Peterse, J.L., Remijnse, P.L., Rodenhuis, S., and Vijver, M.J. Van De, “Breast cancer response to neoadjuvant chemotherapy : predictive markers and relation with outcome,” British journal of cancer 88(3), 406–412 (2003).

[2] Nahleh, Z., Sivasubramaniam, D., Dhaliwal, S., Sundarajan, V., and Komrokji, R., “Residual cancer burden in locally advanced breast cancer : a superior tool,” Current Oncology 15(6), 271–278 (2008).

[3] Rajan, R., Poniecka, A., Smith, T.L., Yang, Y., Frye, D., Pusztai, L., Phil, D., Fiterman, D.J., Gal-gombos, E., et al., “Change in Tumor Cellularity of Breast Carcinoma after Neoadjuvant Chemotherapy As a Variable in the Pathologic Assessment of Response” (2004).

[4] Shelhamer, E., Long, J., and Darrell, T., “Fully Convolutional Networks for Semantic Segmentation” 39(4), 640–651 (2017).

[5] Abadi, M., Agarwal, A., Barham, P., Brevdo, E., Chen, Z., Citro, C., Corrado, G.S., Davis, A., Dean, J., et al., “TensorFlow: Large-scale machine learning on heterogeneous systems” (2015).

[6] Szegedy, C., Vanhoucke, V., Ioffe, S., Shlens, J., and Wonja, Z., “Rethinking the Inception Architecture for Computer Vision,” in IEEE Conf. Comput. Vis. Pattern Recognit., 2818–2826 (2016).

[7] Peikari, M., and Martel, A.L., “Automatic cell detection and segmentation from H&E stained pathology slides using colorspace decorrelation stretching,” in SPIE Med. Imaging, 979114 (2016).